Experimental Study on Behaviour of Stiffened Cold Formed Steel Built Up Hat Section under Flexure by Varying the Depth by Finite Element Analysis

V.Jaya sheela [1] , R.Vijayasarathy[2] , B.Jose Ravindraraj[3]

[1] Asst Professor, Department of Civil Engineering, Ponnaiyah Ramajayam College of Engineering and Technology, and

[2,3] Asst.Professor, Department of Civil Engineering,PRIST UNIVERSITY,Thanjavur,613 403,India.

Abstract: Cold-formed steel is used for many applications in construction of Industrial building. In this experimental work aims at the study of behaviour of built-up hat section with stiffened web and stiffened tension flange under flexure. The finite strip analysis program CUFSM is used to calculate the section and buckling properties of the hat section. Based on these results the cross section and dimensions of the built up section was arrived at and used in this investigation. The flexural tests were conducted on four specimen's built-up hat section with stiffened web and stiffened tension flange. The Data acquisition system with Load cell, Strain Gauge and LVDT are used to record the load, strain and deflection measurements. The numerical simulation of the built up section was performed using Finite element Software ANSYS 12.0. SHELL elastic 4 node 63 elements were used and non linear multi elastic behaviour was considered. In theoretical calculations, strength of beams are calculated using Indian Standard IS: 801-1975, BS 5950-1998 (5). The experimental results are compared with theoretical and numerical analysis results. It is observed that this built up section could be used as a flexural member in structures subjected to light and moderate loads.

Keywords: Built-up hat section, CUFSM, flexural test, Finite element Analysis.

1. Introduction:

Cold-formed steel is used for many applications in construction of Industrial building. In building construction, there are primarily two types of structural steel hot-rolled steel shapes and cold-formed steel shapes. The hot-formed steel shapes are formed at elevated temperatures while the cold- formed steel shapes are formed at room temperature. Cold- formed steel structural members are shapes commonly manufactured from steel plate, sheet are strip material. The manufacturing process involves forming the material by either press- breaking or cold roll-forming to achieve the desired shape. Examples of the cold formed steel are corrugated steel roof and floor decks, steel wall panels, storage racks and steel wall studs. MAHMOOD(2005) et.al studied the performance of locally produced cold formed steel sections for roof truss system. He describes experimental test results of the proposed cold-formed produced locally with the code of practice as prescribed by BS 5950 Part 5 1987 for the use in roof truss system. The tests were also performed to meet [1]the

requirements that have been outlined by Public Works Department, Malaysia. The experimental results showed good agreement with BS 5950 Part 5. From the study it can be concluded that the proposed locally produced cold-formed steel sections and the connections are suitable to be used in the roof truss system provided that the design values should not be more than the experimental values. MAGNUCKI (2010) et.al investigated the elastic buckling of cold-formed thin-walled channel beams with drop flanges. He explained that cold-formed thin-walled channel beams with open Or closed profile of drop flanges as shown. Geometric properties of two C-sections are described including warping functions and warping inertia moments. The analytical solutions of problems of global and local stability of thin-walled beams are presented. The theoretical solutions of elastic buckling problems of these beams are numerically found using FEM and experimentally verified. CHENG YU1 AND BENJAMIN W. SCHAFER (2006) investigated on distortional buckling tests on cold-formed steel beams which demonstrate Failure in cold-formed steel beams is generally initiated by one of three instabilities: local, distortional, or lateral-torsional buckling. For cold-formed steel joists, purlins, or girts, when the compression flange is not restrained by attachment to sheathing or panelling, distortional buckling may be the predominant failure mode. Experimental results on cold-formed steel beams with unrestrained compression flanges are scarce. Therefore a series of distortional buckling tests on cold-formed steel C and Z sections in bending was conducted to establish the capacity in distortional buckling failures. Test details were selected to allow distortional buckling to form, but restrict lateral-torsional buckling to the extent possible. These distortional buckling tests also provide a direct comparison against the local buckling tests previously performed by the writers. As expected, large strength reductions are observed in the tested specimens when distortional buckling initiated the failure instead of local buckling. Based on the results of this study, the Hancock Method for the prediction of distortional buckling strength was the most accurate method for third point braced purlins supporting standing seam roof systems. In addition, a resistance factor was developed to account for the variation between the experimental and the Hancock Method's predicted strengths. The standing seam roof system differs from the conventional through-fastened roof system by the introduction of a clip placed intermediately between the purlin and the decking. Water leakage into a structure is prevented because the clip is embedded into the seam of the deck panels and only fastened to the purlin. However, the advantage the clips provide over water leakage comes at a cost. Unlike the through-fastened system, the introduction of the clips does not allow the steel deck to provide full lateral bracing for the purlins.

2. Experimental Set up

Figure 1 & 2 specimens before testing

Figure 3 Experimental setup

3. METHODOLOGY

This experimental work was carried out by conducting flexural tests on four specimens of built-up hat section with stiffened web (rectangular plate) and stiffened tension flange (triangular shape) having thickness of 1.2mm and length 1500 mm with simply supported end condition. The test program consisted of four specimens with same cross section and varying depth 115 mm, 135 mm, 155 mm, and 175 mm. The vertical stiffeners are connected to the web of specimen by welding. The Data acquisition system with Load cell, Strain Gauge and LVDT are used to record the load, strain and deflection measurements. The finite strip analysis program CUFSM is used to calculate the section and buckling properties of the hat section. The numerical simulation was performed using Finite element Software ANSYS 12.0. SHELL elastic 4 node 63 elements were used and non linear multi elastic behaviour was considered.

<table>
<tr><td>Element Type</td><td colspan="4">SHELL (4 node 63)</td></tr>
<tr><td rowspan="3">Material Property</td><td rowspan="3">Material Model</td><td>Linear</td><td colspan="2">Non Linear</td></tr>
<tr><td>E=2e5</td><td>Yield Stress</td><td>220 MPa</td></tr>
<tr><td>μ=0.3</td><td>Tan. Mod</td><td>2e4 Mpa</td></tr>
<tr><td>Model</td><td colspan="4">Flange width= 120mm,
web = 115 mm, 135 mm, 155 mm, 175 mm
End Stiffener(Lip) =10 mm</td></tr>
<tr><td>Mesh Size</td><td colspan="4">25 mm</td></tr>
<tr><td>Section Thickness</td><td colspan="4">1.2mm</td></tr>
<tr><td>Support Condition</td><td colspan="4">Simply Supported hinged- hinged</td></tr>
</table>

Table 1 Analysis Procedure for stiffened hat Section

4. RESULT AND DISCUSSION

4.1 FLEXURAL TEST: All the specimens were tested for flexural strength under two point loading by using reaction type movable loading frame. Deflection and strain readings are observed from the data logger are listed below.

Specimen	B/D ratio	Ultimate load in kN	Max vertical deflection @ L/3 of span in mm	Max lateral deflection at mid of web in mm
STHAT115B	1	18.602	13.58	-3.36
STHAT135B	0.9	19.519	12.42	-16.55
STHAT155B	0.8	23.451	13.78	-2.9
STHAT175	0.7	24.11	10.32	-6.209

Table 2 Flexure Test Result

4.2 STRESS- STRAIN ON CFS: Strains are measures at the tension flange, compression flange, and web of the specimen using electronic strain gauge. Strain gauge (3mm, 300 ohms) is fixed on the specimen using adhesives. Strain readings are recorded using Data logger and channel connections. The strain readings obtained are listed below.

Specimen	Stress in N/mm^2	Strain in the Compression flange in µmm	Strain in the Tension flange in µmm	Strain in the Web in µmm
STHAT115B	196.620	-21.69	20.11	0.98
STHAT135B	168.053	-88.78	93.78	49.46
STHAT155B	169.531	-85.641	50.341	55.692
STHAT175	148.565	-295.336	270.561	284.047

Table 3 Stress Strain Values

4.3 FLEXURE TEST ON STIFFENED CFS BUILT UP SECTIONS

Load -Deflection and Stress - Strain plot has been drawn for all the specimens from the experimental data. The behaviour of the specimens are compared from the below plots. Ultimate load, failure pattern, specimen behaviour against flexural loading and their characteristics are determined from the results and plots.

Specimen	B/D ratio	Ultimate load in kN	Max deflection @ L/3 of span in mm	% Increase in Ultimate load
STHAT115B	1	18.602	13.58	-
STHAT135B	0.9	19.519	12.42	4.93
STHAT155B	0.8	23.45	13.78	26.06
STHAT175B	0.7	24.55	10.32	31.97

Table 4 Flexural Capacity of Sections

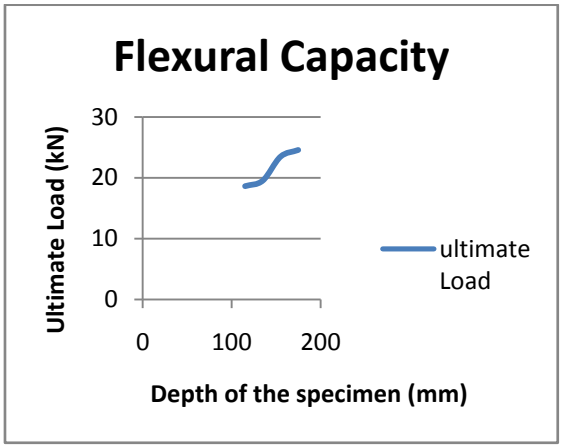

Figure 4 Flexural Capacity

Comparing the flexure test results shown in the above table, it is observed that the Built-up section with height 175 mm has 32 % higher ultimate load carrying capacity than the other specimens with lesser depth. Above table and chart clearly shows the influence of aspect ratio in increase of ultimate load.

4.4 STIFFNESS: Stiffness may be defined as the load required to cause unit deflection. The stiffness values of the specimen at ultimate load were presented in the table and the graph is plotted . The percentage increase in the stiffness values were shown in the table.

Specimen	B/D ratio	Ultimate load in kN	Max deflection @ L/3 of span in mm	Stiffness (kN/mm)
STHAT115B	1	18.602	13.58	1.36
STHAT135B	0.9	19.519	12.42	1.59
STHAT155B	0.8	23.45	13.78	1.70
STHAT175	0.7	24.55	10.32	2.84

Table 5 Stiffness of Sections

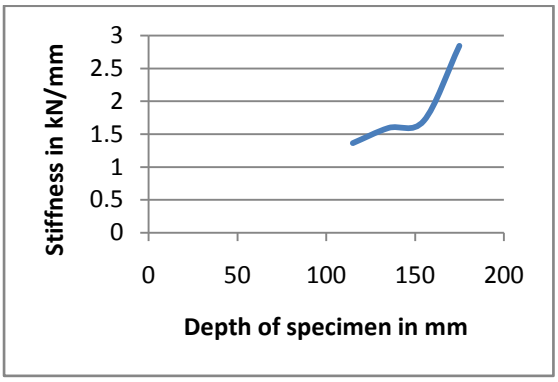

Figure 5 Stiffness of the specimen

From the above graph, it was observed that the stiffness of the specimen also increases as the depth of the specimen increases.

4.5 LOAD VS DEFLECTION PLOTS

AC LVDT were used to measure deflection for the specimens at L/3rd from of the span length (i.e under the point load) and mid of the web. Figure 6 & 7 shows the load vs deflection curve from the experimental results of stiffened CFS built up section.

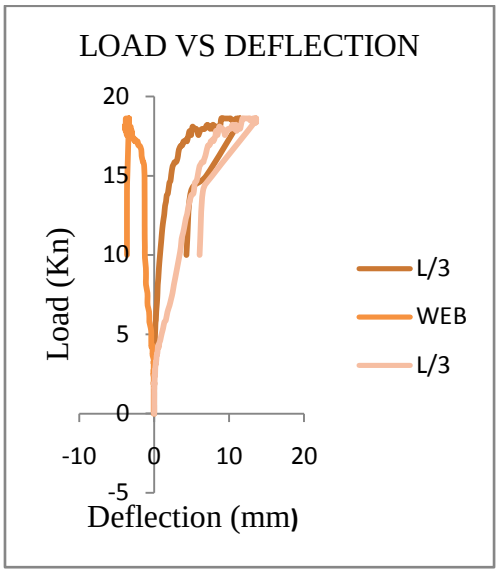

Figure 6 load vs deflection for STHAT115B

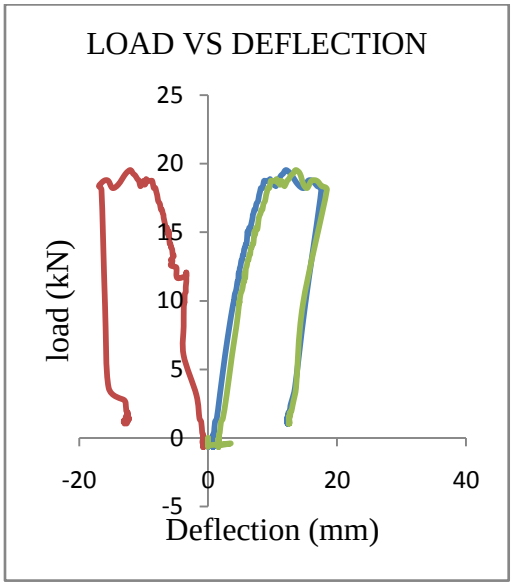

Figure 7 load vs deflection curve STHAT135B

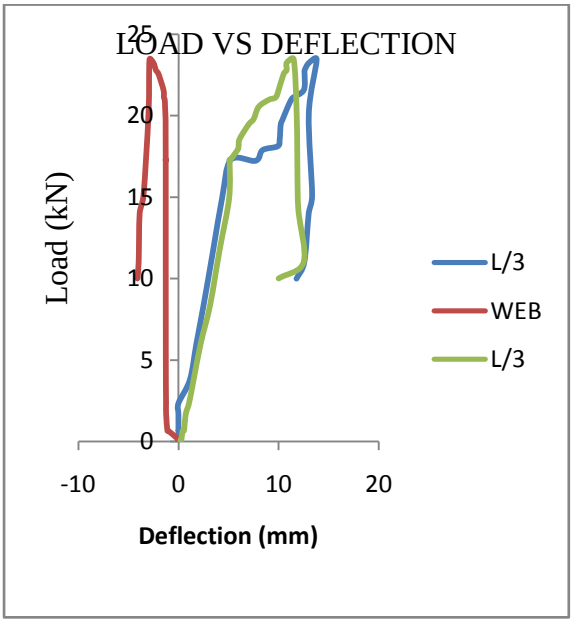

Figure 8 load vs deflection curve for STHAT155B

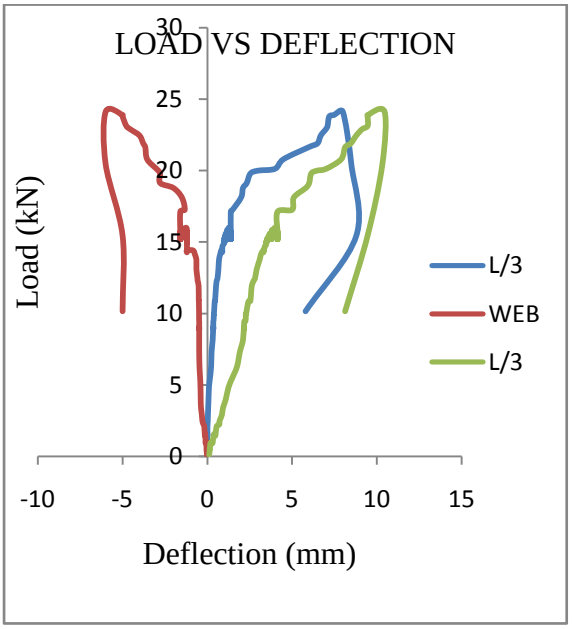

Figure 9 load vs deflection curve for STHAT175B

From the above graphs, it is observed that as the load increases the deflection increases and it decreases as the load is decreased after reaching its maximum limit showing the elastic property of the material. The curve for the web portion lies in the negative region as while loading the web moved away from the LVDT due to the distortional buckling.

4.6 STRESS STRAIN BEHAVIOR

Strain was measured at the compression flange, tension flange, and web of the specimen by using electronic strain gauge. Strain gauge used here is of 300 ohm resistance and 3mm thick. When the specimen is loaded in flexure, two observations are made on the stress strain curve. For all the four specimens the behavior is more or less linear up to certain limit which obeys Hooks law and then the curve is significantly non-linear and reaches its peak at the maximum sustainable stress. The following plot shows the stress strain plot for the four specimens.

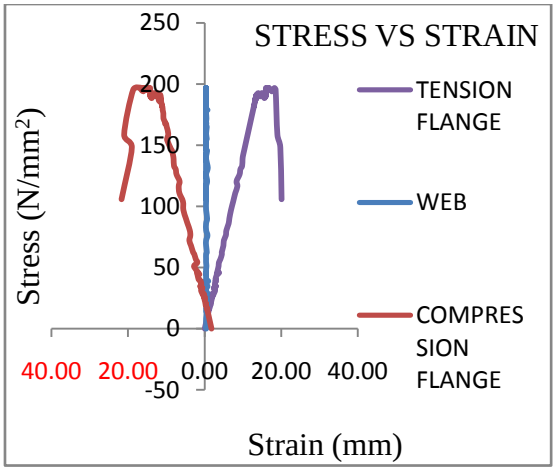

Figure 10 Stress vs Strain for STHAT115B

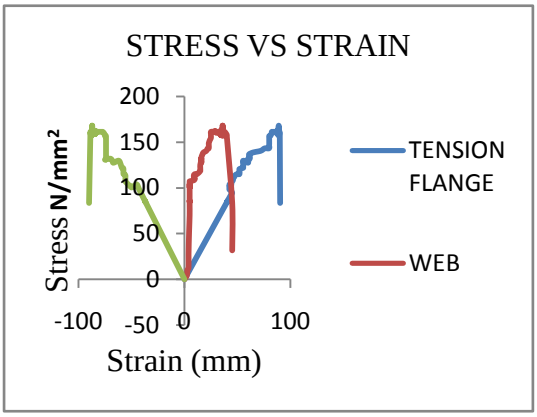

Figure 11 Stress vs Strain for STHAT135B

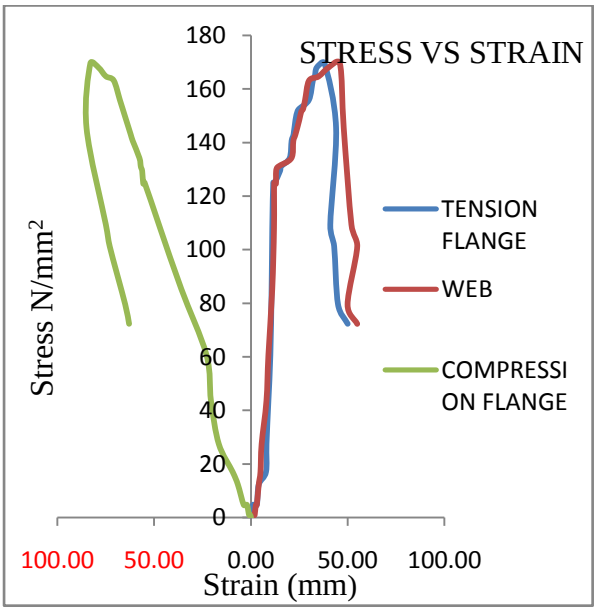

Figure 12 Stress vs Strain for STHAT155B

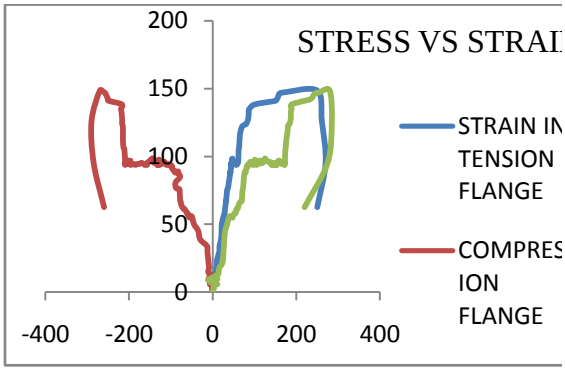

Figure 13 Stress vs Strain from STHAT175B

MODES OF FAILURE

From the results of the experimental and model analysis, failure modes of the specimens are discussed. Pictorial view of failure pattern observed from the model analysis and experimental work are presented below,

- As the specimens are built up sections the major failure expected here is joint failure between the top and bottom flange with the vertical web, but the above mentioned failure didn't took place because the spot welding at regular intervals between the flange and web plates provides efficient joint between the assembled plates.
- Failure of the specimen occurs when the specimen buckles under the loading.
- In the specimen, STHAT115B, Local buckling occurs at the compression flange and lip.
- Failure pattern differs as the depth of the specimen increases. Initially at lower depth, the failure is mainly due to local buckling of flange plates under the point of loading. In the specimen STHAT155,

both local and distortional buckling occurs.

- In the case of STHAT175, the specimen undergoes flexural torsional buckling in addition to distortion, but after removal of load the specimen regain its original shape

The following pictures show some of the failures in the specimens,

Figure 14 Buckling under the loading point

Figure 15 Buckling of the vertical stiffener under the loading point

Figure 16 Torsional buckling of STHAT155B

5. COMPARISON OF RESULTS

Comparison of the load obtained from the theoretical, numerical and experimental results.The failure pattern obtained from the numerical analysis (ANSYS) matches with the experiment and it is shown below,

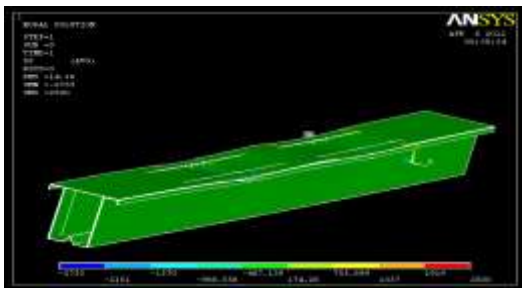

Figure 17 Buckling under the loading point

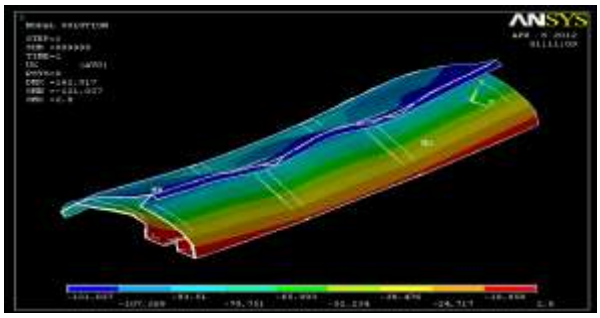

Figure 18 Distortional buckling

Figure 19 Buckling of the vertical stiffener under the loading point

6. CONCLUSION

- Failure modes of the specimen vary as the (B/D) ratio decreases i.e. buckling of flange plates to distortional buckling of web plates.
- Ultimate moment carrying capacity increases as the depth increases. But due to the occurrence of distortional buckling the percentage increase is less. This could be rectified by further stiffening the web.
- Spot welding at regular intervals between the web plates and stiffener plates provides efficient joint.
- Vertical stiffener provided in web is not efficient as horizontal stiffener. Finite element model can be used for further studies to develop the shape and location of the stiffener.
- Experimental results show that the failure of the section occurs mainly due to the buckling of flange plates and torsional buckling. Finite element analysis also shows the same failure pattern.
- By increasing the thickness of the specimen, the load carrying capacity will get increased and in turn its other behaviour also gets improved.
- This section could be used as a structural member and as beam supporting a composite slab.

ACKNOWLEDGEMENT

We express sincere thanks to our Beloved Principal Prof. M. Abdul Ghani Khan, Ponnaiyah Ramajayam College of Engineering and Technology, Thanjavur for given valuable suggestions and Motivate this Efforts.

REFERENCES

1.Hancock, G.J., Merrick, J.T., and Bambach, M.R., (1998), "Distortional BucklingFormulae for Thin Walled Channel and Z-Sections with Return Lips," Proceedings of the Fourteenth International Specialty Conference on Cold-Formed Steel Structures, St. Louis, MO., October 15-16.

2.Hancock, G.J., (1985), "Distortional Buckling of Steel Storage Rack Columns," Journal of Structural Engineering, ASCE, Vol. 111, No. 12, pp. 2770-2783.

3.Hancock, G.J., (1994), "Design of Cold-Formed Steel Structures (to Australian Standard. AS 1538-1988) 2nd Edition," Australian Institute of Steel Construction, Sydney, Australia, pp. 38.

4.Hancock, G.J., (1997), "Design for Distortional Buckling of Flexural Members," Thin-Walled Structures, Vol. 27, No. 1, pp. 3-12.

5. Hancock, G.J., and Lau, S.C.W., (1986), "Distortional Buckling Formula for Thin-Walled Channel Columns," Research Report No. R-521, School of Civil and Mining Engineering, University of Sydney, Sydney, Australia.

6. Hancock, G.J., and Lau, S.C.W., (1987), "Distortional Buckling Formulas for Channel Columns," Journal of Structural Engineering, ASCE, Vol. 113, No. 5, pp.1063-1078.

7. Hancock, G.J., and Lau, S.C.W., (1990), "Inelastic Buckling of Channel Columns in the Distortional Mode," Thin-Walled Structures, Vol. 10, pp. 59-84.

8.Hancock, G.J., Rogers, C.A., and Schuster, R.M., (1996), "Comparison of the Distortional Buckling Method for Flexural Members with Tests," Proceedings of the Thirteenth International Specialty Conference on Cold-Formed Steel Structures, St. Louis, MO, October 17-18.

9.Hancock, G.J., (1998), Design of Cold-Formed Steel Structures, 3rd Edition, Australian Institute of Steel Construction, North Sydney, Australia.